

Photon-assisted electron transport in graphene

B. Trauzettel,¹ Ya. M. Blanter,² and A. F. Morpurgo²

¹*Instituut-Lorentz, Universiteit Leiden, P.O. Box 9506, 2300 RA Leiden, The Netherlands*

²*Kavli Institute of Nanoscience, Delft University of Technology, Lorentzweg 1, 2628 CJ Delft, The Netherlands*

(Dated: June 2006)

Photon-assisted electron transport in ballistic graphene is analyzed using scattering theory. We show that the presence of an ac signal (applied to a gate electrode in a region of the system) has interesting consequences on electron transport in graphene, where the low energy dynamics is described by the Dirac equation. In particular, we discuss a feasible way to generate an electron wave function in graphene that contains solutions to the Dirac equation at different energies. Such a wave function is essential to see evidence of *zitterbewegung* of relativistic fermions. We show, however, that an oscillating current as a consequence of this wave function is not sufficient to prove the presence of *zitterbewegung* in graphene, because of its similarity to the corresponding transport problem based on the Schrödinger equation. In the dc limit of photon-assisted transport, *zitterbewegung* is certainly not directly observable. However, sharp steps appear in dG/dV (as a function of bias V), where G is the differential conductance. This is a distinct signature of ballistic transport of Dirac electrons and can be used as a spectrometer for finite frequency noise.

PACS numbers: 73.23.Ad, 73.23.-b, 73.63.-b, 03.65.Pm

Since the discovery of an anomalous quantum Hall effect in graphene (a single layer of carbon atoms) [1, 2], promising possibilities to observe quantum dynamics of Dirac fermions in such systems have been proposed. The most prominent one is the quantum-limited conductivity (of order e^2/h), where measurements [1, 2] and theoretical predictions [3, 4, 5, 6] are still inconsistent with each other. Other examples of unusual quantum transport phenomena in graphene are a maximum Fano factor (ratio of noise power and mean current) of $\frac{1}{3}$ [7], selective transmission of Dirac electrons through n - p junctions [8], the phenomenon of Klein tunnelling (related to transport through electrostatic barriers) [9], and specular Andreev reflections at an interface between graphene and a superconductor [10]. Recently, the effect on the longitudinal and Hall conductivity of an applied microwave signal has been analyzed in bulk graphene [11]. All these works exploit modifications, even though in an unexpected fashion, of effects previously described for fermions obeying the Schrödinger equation. An example of a novel effect, present for Dirac fermions but absent for Schrödinger fermions, is *zitterbewegung* (ZB) [12, 13]. It manifests itself, for instance, in a time-dependent oscillation of the position operator of a Dirac electron in the Heisenberg picture. A pioneering attempt to describe an experimental way to observe ZB in III-V semiconductor quantum wells has been made in Ref. [14]. Others have adopted this idea to carbon nanotubes [15], spintronic, graphene, and superconducting systems [16]. What is missing in Refs. [14, 15, 16] – related to the detection of ZB in solid-state systems – is to show that an unambiguous signature of ZB exist, which is qualitatively different from the corresponding Schrödinger case (where ZB is absent). We demonstrate below that such a comparison is absolutely crucial in order to prove the existence of ZB in solid-state systems governed by the Dirac equation (DE).

An essential prerequisite to observe ZB is to generate

a state which is a superposition of positive and negative energy solutions to the DE [13]. We show that it is feasible to generate such a state in a region of graphene by applying an ac signal to a neighboring region of graphene and a bias to allow electron transport from the one region to the other (see Fig. 1). Such a setup corresponds to the Tien-Gordon problem of photon-assisted electron transport for Dirac electrons [17, 18]. We call the region to which the ac signal is applied $Gr(\text{ac})$ and the neighboring region in which a superposition of positive and negative energy solutions to the DE is injected $Gr(\text{in})$. The ac signal stimulates the absorption and emission of photons, which in turn lead to a population of different side bands around the Fermi energy [18]. Then, the resulting electron field operator in region $Gr(\text{in})$ is precisely what is needed to observe ZB in graphene. However, we show that the detection of an oscillating current is not sufficient to prove the existence of ZB in graphene. The reason is that a preparation of a state that is a superposition of different energy solutions to the Schrödinger equation also yields an oscillating current. Thus, in order to observe ZB in graphene, one needs to be specific about what are really intrinsic and unambiguous signatures of ZB in a given experimental geometry.

In the dc limit, ZB is not directly observable but photon-assisted electron transport in graphene still contains interesting fingerprints of the underlying relativistic quantum dynamics of low energy excitations. The special transmission properties of Dirac electrons in graphene yield, for instance, an unusual dependence of the non-linear differential conductance on the applied bias. Resonance phenomena (sharp steps in dG/dV , where $G = dI/dV$ is the differential conductance) should be observable if the applied bias V equals multiples of the applied ac frequency ω . These resonance phenomena are due to the vanishing of propagating modes directly at the Dirac point (the point in the spectrum of graphene,

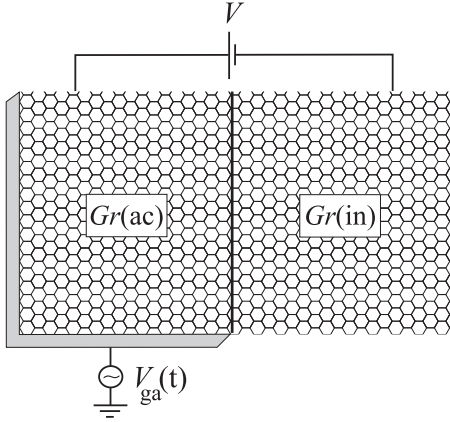


FIG. 1: Schematic of the setup. Two regions of graphene (called $Gr(ac)$ and $Gr(in)$) are voltage-biased with respect to each other with a bias V . A gate electrode (grey-shaded area) shifts the Dirac point of region $Gr(ac)$ away from zero energy. Additionally a small ac signal is applied to the gate to generate side band transitions (as described in the text). The applied gate voltage $V_{ga}(t)$ has to be chosen in such a way that the (time-dependent) chemical potential in region $Gr(ac)$ is given by $\mu(x < 0) = eV_S + eV_{ac} \cos(\omega t)$.

where the valence band and the conduction band touch each other) and, therefore, a signature of coherent dynamics of Dirac fermions. This implies an interesting application of graphene: It can be used as a spectrometer for high frequency noise – similar to the superconductor-insulator-superconductor (SIS) junction in Ref. [19] with the advantage that there is no frequency limit.

The setup under consideration is illustrated in Fig. 1. It contains two regions of graphene called $Gr(ac)$ and $Gr(in)$. A gate electrode in region $Gr(ac)$ shifts the Dirac points of the two regions with respect to each other by an amount eV_S (which distinguishes the two regions of graphene). Additionally, we apply a small ac signal to the gate electrode.

An ideal sheet of graphene (in the absence of K - K' inter-valley mixing) can be described in the effective mass approximation by a two-dimensional DE for a two-component wave-function envelope $\Psi = (\Psi_1, \Psi_2)$ (subscript 1, 2 refers to pseudospins, whose origin can be traced to the presence of two carbon sublattices)

$$\left[-iv\hbar \begin{pmatrix} 0 & \partial_x - i\partial_y \\ \partial_x + i\partial_y & 0 \end{pmatrix} - \mu(x) \right] \Psi_{e/h} = i\hbar \partial_t \Psi_{e/h}, \quad (1)$$

where v is the Fermi velocity [22]. The index e/h refers to electron-like (energy $\varepsilon > 0$ with respect to the Dirac point) and hole-like (energy $-\varepsilon < 0$ with respect to the Dirac point) solutions to the DE. The chemical potential of the two regions $Gr(ac)$ ($x < 0$) and $Gr(in)$ ($x > 0$) is

$$\mu(x) = \begin{cases} eV_S + eV_{ac} \cos(\omega t), & \text{for } x < 0 \\ 0, & \text{for } x > 0 \end{cases} . \quad (2)$$

Let us first explain the signature of ZB in the current in the absence of $\mu(x)$ and then show why our particular choice (2) has been made. In the absence of the potential $\mu(x)$, the time evolution of the electron field operator that obeys Eq. (1) (with $\mu(x) = 0$) can be written as

$$\Psi_{\mathbf{p}}(t) = \frac{1}{2} [\Psi_{\mathbf{p}}^{(+)}(t) + \Psi_{\mathbf{p}}^{(-)}(t)] \quad (3)$$

with $\mathbf{p} = (p_x, p_y)$, $p = \sqrt{p_x^2 + p_y^2}$, and

$$\Psi_{\mathbf{p}}^{(\pm)}(t) = e^{\mp i v p t / \hbar} (1 \pm (\mathbf{p} \cdot \vec{\sigma})/p) \Psi_{\mathbf{p}},$$

where $\vec{\sigma} = (\sigma_x, \sigma_y)$ is a vector of Pauli matrices. A straightforward calculation of the current operator in the Heisenberg picture [6] shows that an oscillatory component in time exists due to an interference of $\Psi_{\mathbf{p}}^{(+)}(t)$ and $\Psi_{\mathbf{p}}^{(-)}(t)$ solutions of the DE. Therefore, in order to see a signature of ZB in the current, it is important that electron-like and hole-like solutions interfere. More generally, an oscillatory component of the current arises if the electron field operator contains solutions to the DE at different energies. Consequently, if we calculated the current operator corresponding to a solution to the DE with a fixed energy ε , then there would be no oscillatory component of the current operator left and, thus, no sign of ZB in the current. Importantly, this is the general situation in ballistic transport in graphene if a plane wave solution (of a particle with energy ε) to the DE is injected from one region to another. Thus, ballistic dc transport in graphene shows no direct sign of ZB.

However, there is a feasible way to inject a state which has a similar structure as the one in Eq. (3) (necessary to see signatures of ZB) into a region of graphene. The idea is to apply a small ac signal to the gate shown in Fig. 1. The solution to the wave equation (1) for $x < 0$ (in region $Gr(ac)$) may then be written as

$$\begin{aligned} \Psi_{e/h}^{(ac)}(\vec{x}, t) &= \Psi_{0,e/h}^{(ac)}(\vec{x}, t) e^{-i(eV_{ac}/\hbar\omega) \sin(\omega t)} \\ &= \sum_{m=-\infty}^{\infty} J_m \left(\frac{eV_{ac}}{\hbar\omega} \right) \Psi_{0,e/h}^{(ac)}(\vec{x}, t) e^{-im\omega t}, \end{aligned} \quad (4)$$

where $\Psi_{0,e/h}^{(ac)}(\vec{x}, t) = \Psi_{0,e/h}^{(ac)}(\vec{x}) e^{\mp i \varepsilon t / \hbar}$ and

$$\left[-iv\hbar \begin{pmatrix} 0 & \partial_x - i\partial_y \\ \partial_x + i\partial_y & 0 \end{pmatrix} - eV_S \right] \Psi_{0,e/h}^{(ac)} = \pm \varepsilon \Psi_{0,e/h}^{(ac)}. \quad (5)$$

(We have dropped the argument \vec{x} of the wave function in the latter equation.) In Eq. (4), J_m is the m th order Bessel function. From now on, we focus without loss of generality on electron-like solutions only and drop the index e . This is justified because, in ballistic transport from one region of graphene to another region, particles with a fixed energy ε (which can be either positive or negative with respect to the Dirac point) are transmitted and their energy is conserved in the absence of inelastic scattering. However, the desired state – a superposition

of positive and negative energy solutions to the DE – is then generated by the presence of the different side bands m which come with phase factors $e^{-im\omega t}$ that shift the center energy ε by integer multiples of $\hbar\omega$.

The electron-like plane wave solutions of Eq. (5) can be written as linear combinations of the basis states [10]

$$\Psi_{0,+}^{(\text{ac})} = \frac{e^{iqy+i k_{\text{ac}} x}}{\sqrt{\cos \alpha_{\text{ac}}}} \begin{pmatrix} e^{-i\alpha_{\text{ac}}/2} \\ e^{i\alpha_{\text{ac}}/2} \end{pmatrix}, \quad (6)$$

$$\Psi_{0,-}^{(\text{ac})} = \frac{e^{iqy-i k_{\text{ac}} x}}{\sqrt{\cos \alpha_{\text{ac}}}} \begin{pmatrix} e^{i\alpha_{\text{ac}}/2} \\ -e^{-i\alpha_{\text{ac}}/2} \end{pmatrix}, \quad (7)$$

where

$$\alpha_{\text{ac}} = \arcsin \left(\frac{\hbar v q}{\varepsilon + e V_S} \right), \quad (8)$$

q is the transversal momentum, and $k_{\text{ac}} = (\varepsilon + e V_S) \cos \alpha_{\text{ac}} / (\hbar v)$ the longitudinal momentum in region $Gr(\text{ac})$. Likewise, electron-like plane wave solutions of Eq. (1) in region $Gr(\text{in})$ can be written as linear combinations of the basis states

$$\Psi_{0,+}^{(\text{in})} = \frac{e^{iqy+i k_{\text{in}} x}}{\sqrt{\cos \alpha_{\text{in}}}} \begin{pmatrix} e^{-i\alpha_{\text{in}}/2} \\ e^{i\alpha_{\text{in}}/2} \end{pmatrix}, \quad (9)$$

$$\Psi_{0,-}^{(\text{in})} = \frac{e^{iqy-i k_{\text{in}} x}}{\sqrt{\cos \alpha_{\text{in}}}} \begin{pmatrix} e^{i\alpha_{\text{in}}/2} \\ -e^{-i\alpha_{\text{in}}/2} \end{pmatrix} \quad (10)$$

with $\alpha_{\text{in}} = \arcsin(\hbar v q / \varepsilon)$ and $k_{\text{in}} = (\varepsilon / \hbar v) \cos \alpha_{\text{in}}$. Now, we solve the transmission problem from region $Gr(\text{ac})$ to region $Gr(\text{in})$. An incoming wave function from region $Gr(\text{ac})$ is given by

$$\Psi_i^{(\text{ac})}(\vec{x}, t) = \sum_{m=-\infty}^{\infty} J_m \left(\frac{e V_{\text{ac}}}{\hbar \omega} \right) \Psi_{0,+}^{(\text{ac})} e^{-i(\varepsilon + \hbar m \omega)t/\hbar}.$$

The reflected wave function in region $Gr(\text{ac})$ reads

$$\Psi_r^{(\text{ac})}(\vec{x}, t) = \sum_{m=-\infty}^{\infty} r_m J_m \left(\frac{e V_{\text{ac}}}{\hbar \omega} \right) \Psi_{0,-}^{(\text{ac})} e^{-i(\varepsilon + \hbar m \omega)t/\hbar},$$

where r_m is the energy-dependent reflection coefficient. Furthermore, a transmitted wave function in region $Gr(\text{in})$ can be written as

$$\Psi_{\text{tr}}^{(\text{in})}(\vec{x}, t) = \sum_{m=-\infty}^{\infty} t_m J_m \left(\frac{e V_{\text{ac}}}{\hbar \omega} \right) \Psi_{+,m}^{(\text{in})} e^{-i(\varepsilon + \hbar m \omega)t/\hbar}, \quad (11)$$

where

$$\Psi_{+,m}^{(\text{in})}(\vec{x}) = \frac{e^{iqy+i k_{\text{in},m} x}}{\sqrt{\cos \alpha_{\text{in},m}}} \begin{pmatrix} e^{-i\alpha_{\text{in},m}/2} \\ e^{i\alpha_{\text{in},m}/2} \end{pmatrix} \quad (12)$$

with

$$\alpha_{\text{in},m} = \arcsin \left(\frac{\hbar v q}{\varepsilon + \hbar m \omega} \right) \quad (13)$$

and $k_{\text{in},m} = (\varepsilon + \hbar m \omega) \cos \alpha_{\text{in},m} / (\hbar v)$. In Eq. (11), t_m is the energy-dependent transmission coefficient. In order to determine t_m and r_m , we need to match wave functions at $x = 0$, namely

$$\Psi_i^{(\text{ac})}(x = 0, y, t) + \Psi_r^{(\text{ac})}(x = 0, y, t) = \Psi_{\text{tr}}^{(\text{in})}(x = 0, y, t).$$

The solutions to the resulting set of equations are

$$r_m = \frac{e^{i\alpha_{\text{ac}}} - e^{i\alpha_{\text{in},m}}}{1 + e^{i(\alpha_{\text{ac}} + \alpha_{\text{in},m})}}, \quad (14)$$

$$t_m = e^{-i(\alpha_{\text{ac}} - \alpha_{\text{in},m})/2} \sqrt{\frac{\cos \alpha_{\text{in},m}}{\cos \alpha_{\text{ac}}}} \frac{1 + e^{2i\alpha_{\text{ac}}}}{1 + e^{i(\alpha_{\text{ac}} + \alpha_{\text{in},m})}},$$

where α_{ac} is given by Eq. (8) and $\alpha_{\text{in},m}$ by Eq. (13). It is easy to verify that unitarity holds $|r_m|^2 + |t_m|^2 = 1$. Furthermore, Eq. (14) shows that if the angle of incidence is zero ($q = 0$) then all transmission coefficients are 1 and all reflection coefficients vanish. This is known as Klein tunnelling in relativistic quantum dynamics [9].

In order to calculate the transmitted current, we need to calculate the current density operator in x -direction $J_x(\vec{x}, t) = ev\Psi^*(\vec{x}, t)\sigma_x\Psi(\vec{x}, t)$, integrate over a cross section in y -direction, and over angles of incidence. In the following, we assume that a dc bias V is applied between regions $Gr(\text{ac})$ and $Gr(\text{in})$ and that $k_B T$ is the lowest of all energy scales. The average current is then given by

$$I = \frac{4eW}{h\pi} \int_0^{q_{\text{max}}} dq \int_0^{eV} d\varepsilon \sum_{m,m'=-\infty}^{\infty} \times J_m \left(\frac{e V_{\text{ac}}}{\hbar \omega} \right) J_{m'} \left(\frac{e V_{\text{ac}}}{\hbar \omega} \right) t_m^* t_{m'} e^{i(m-m')\omega t}, \quad (15)$$

where W is the width of the sample and $q_{\text{max}} = \min\{|eV + \hbar m \omega|/\hbar v, |eV + eV_S|/\hbar v\}$ is the upper bound of the transversal momentum of propagating modes [23]. A factor 4 has been added to the right hand side of Eq. (15) to take into account for spin and valley degeneracy. Apparently, there are terms in Eq. (15) that do not depend on time (where $m = m'$) and terms that oscillate as a function of time (where $m \neq m'$). The latter terms bear a resemblance to the terms in the current that are attributed to ZB [6], which is due to the fact that both arise from interferences of solutions to the DE at different energies. However, the bare existence of the oscillating terms cannot be regarded as a proof of ZB in graphene. The reason is that a preparation of a state that is a superposition of different energy solutions to the Schrödinger equation also yields an oscillating current like Eq. (15) [18].

Nevertheless, Eq. (15) contains interesting fingerprints of the underlying relativistic quantum dynamics which even remain in the dc limit. In that limit, only terms with $m = m'$ survive in Eq. (15) and the differential conductance reads

$$G = \frac{4e^2 W}{h\pi} \int_0^{q_{\text{max}}} dq \sum_{m=-\infty}^{\infty} J_m^2 \left(\frac{e V_{\text{ac}}}{\hbar \omega} \right) |t_m(\varepsilon = eV)|^2. \quad (16)$$

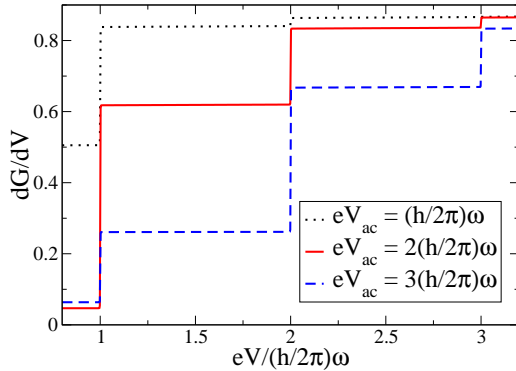


FIG. 2: (color online). dG/dV is plotted in units of $8e^3W/(vh^2)$ for a fixed value of $eV_s/\hbar\omega = 100$ and different values of $eV_{ac}/\hbar\omega$. Sharp steps appear when the applied bias equals multiples of the ac frequency. The size of the steps is non-universal. It depends on the weight of the different side bands given by the Bessel functions in Eq. (16). For the given values of $eV_{ac}/\hbar\omega$, it is sufficient to include side bands up to $|m| = 4$ to calculate dG/dV to a very high accuracy.

We now show that distinct features arise from the energy-dependence of the scattering matrix – typical for graphene. As illustrated in Fig. 2, steps appear in dG/dV if the bias V equals multiples of the ac frequency ω . The steps show up whenever the number of propagating modes in a side band m vanishes. That is when the corresponding energy of charge carriers hits the Dirac point, where the density of states vanishes. The magnitude of the steps depends on the weight of the different side bands (given by the Bessel functions) and is non-universal. Nevertheless, the appearance of these steps can be used as a detector for finite frequency noise, similar to the SIS junction used in Ref. [19]. The advantage

of graphene as a finite frequency noise detector is that a graphene detector has no frequency limit, whereas the SIS detector is limited by the size of the superconducting gap.

At this point, we mention that our results are obtained using scattering theory of non-interacting Dirac fermions. As shown by Pedersen and Büttiker [20] (for the corresponding problem based on the Schrödinger equation) screening of near-by gates can change the predictions of a scattering theory based on non-interacting particles. Although screening is expected to be reduced close to the Dirac point in graphene [21], where the interesting predictions illustrated in Fig. 2 appear, a careful analysis of mesoscopic ac transport in graphene in the presence of screening by near-by gates is an interesting extension of the research done here.

In conclusion, we have shown that the essential condition to see ZB in graphene is to generate a state with positive and negative energy solutions to the DE. In mesoscopic graphene, this can be done in a feasible way by applying a microwave signal to one region of graphene and a bias between that region and a neighboring region. The resulting electron state contains the desired superposition of wave functions that solve the DE at different energies, which manifests itself as an oscillating contribution to the current. However, the observation of such an oscillating current alone is not sufficient to prove the existence of ZB in graphene because the corresponding transport problem based on the Schrödinger equation is similar. Nevertheless, interesting features remain in the photon-assisted transport through graphene. Therefore, we propose to use graphene as a spectrometer for finite frequency noise.

We thank C.W.J. Beenakker, H. Heersche, P. Jarillo-Herrero, J. Schliemann, I. Snyman, and L.M.K. Vandersypen for interesting discussions. This research was supported by the Dutch Science Foundation NWO/FOM.

[1] K. S. Novoselov, *et al.*, *Nature* **438**, 197 (2005).
[2] Y. Zhang, *et al.*, *Nature* **438**, 201 (2005).
[3] A. W. W. Ludwig, *et al.*, *Phys. Rev. B* **50**, 7526 (1994).
[4] K. Ziegler, *Phys. Rev. Lett.* **80**, 3113 (1998).
[5] N. M. R. Peres, F. Guinea, and A. H. Castro Neto, *Phys. Rev. B* **73**, 125411 (2006).
[6] M. I. Katsnelson, *Eur. Phys. J. B* **51**, 157 (2006).
[7] J. Tworzydlo, *et al.*, cond-mat/0603315.
[8] V. V. Cheianov and V. I. Falko, cond-mat/0603624.
[9] M. I. Katsnelson, K. S. Novoselov, and A. K. Geim, cond-mat/0604323.
[10] C. W. J. Beenakker, cond-mat/0604594.
[11] V. P. Gusynin, S.G. Sharapov, and J. P. Carbotte, cond-mat/0603267.
[12] E. Schrödinger, *Sitzungsber. Preuss. Akad. Wiss., Phys. Math. Kl.* **24**, 418 (1930).
[13] K. Huang, *Am. J. Phys.* **20**, 479 (1952).
[14] J. Schliemann, D. Loss, and R. M. Westervelt, *Phys. Rev. Lett.* **94**, 206801 (2005); *Phys. Rev. B* **73**, 085323 (2006).
[15] W. Zawadzki, cond-mat/0510184; T. M. Rusin and W. Zawadzki, cond-mat/0605384.
[16] J. Cserti and G. David, cond-mat/0604526.
[17] P. K. Tien and J. P. Gordon, *Phys. Rev.* **129**, 647 (1963).
[18] G. Platero and R. Aguado, *Phys. Rep.* **395**, 1 (2004).
[19] R. Deblock, *et al.*, *Science* **301**, 203 (2003).
[20] M. H. Pedersen and M. Büttiker, *Phys. Rev. B* **58**, 12993 (1998).
[21] D. P. DiVincenzo and E. J. Mele, *Phys. Rev. B* **29**, 1685 (1984).
[22] The dimensions of the sample are assumed to be large enough such that boundary effects can be neglected.
[23] The bias is applied such that the Fermi function (at zero temperature) in region $Gr(ac)$ reads $f_{ac}(E) = \theta(eV - E)$ and, in region $Gr(in)$, $f_{in}(E) = \theta(-E)$, where $\theta(x)$ is the Heaviside step function. Since the scattering matrix is energy-dependent, the current I depends on the way the bias is applied and not just on its magnitude V .